PHILOSOPHICAL TRANSACTIONS OF THE ROYAL SOCIETY A

Phil. Trans. R. Soc. A (2012) **370**, 2930–2948
doi:10.1098/rsta.2011.0220

Review

The memory of surfaces: epitaxial growth on quasi-crystals

By R. McGrath[1,*], H. R. Sharma[1], J. A. Smerdon[2] and J. Ledieu[3]

[1]*Surface Science Research Centre and Department of Physics, The University of Liverpool, Liverpool L69 3BX, UK*
[2]*Center for Nanoscale Materials, Argonne National Laboratory, 9700 South Cass Avenue, Argonne, IL 60439 USA*
[3]*Institut Jean Lamour, UMR7198 CNRS Nancy-Université-UPVM, Ecole des Mines, Parc de Saurupt, 54042 Nancy, France*

If crystal structures can be viewed as repositories of information, then crystal surfaces offer a pathway by which this information can be used to grow new structures through the process of epitaxy. The information transfer process is one of self-organization, and the kinetic and energetic factors influencing this are complex. They include the relative strengths of the adsorbate–adsorbate and adsorbate–substrate interactions, the flux of incoming species and the temperature of the system. In this brief review, we explore how the interplay of these factors influences the degree to which the epitaxial structures retain the 'memory' of the template, illustrating the discussion with examples from epitaxy on quasi-crystal surfaces.

Keywords: bismuth; aluminium–palladium–manganese; scanning tunnelling microscopy; quasi-crystal; surface; adsorption

1. Introduction

The relationship between structure and information has been an enduring theme of the research career of Alan L. Mackay. Appropriately, several of the contributions to this volume are concerned with processes of information transfer to and from molecular or crystalline structures. The information may be encoded in a variety of different ways, for example, in the optical lattice described by Vishveshwara [1]. In that case, the resulting structure is the atomic Bose–Einstein condensate. Alternatively, the information is contained in biological molecules such as DNA [2] or peptides and RNA [3], and a new structure is generated or replicated through biological processes. Another possibility is that the information may be contained within the structural elements or building blocks themselves, and the new structure is generated through a process of

*Author for correspondence (mcgrath@liv.ac.uk).

One contribution of 14 to a Theme Issue 'Beyond crystals: the dialectic of materials and information'.

Table 1. A brief listing and explanation of some terms associated with epitaxy.

epitaxy:	the process of depositing a monocrystalline film on a monocrystalline substrate
homoepitaxy:	a type of epitaxy in which a single-crystal layer is grown on a substrate of the same material
heteroepitaxy:	a type of epitaxy in which a single-crystal layer is grown on a substrate of different material that has a compatible crystal structure
rotational epitaxy:	growth of one crystal on the surface of another crystal in which the growth of the deposited crystal is oriented by the lattice structure of the substrate
pseudomorphic growth:	growth of a structure that has an uncharacteristic crystalline form as a result of assuming the structure of another crystal that has been used as a template

self-assembly [4]. In this paper, we consider crystal structures as repositories of information. Their surfaces then offer an interface whereby this information may be exploited. The process of information transfer in this case is through self-assembled growth, a process commonly termed as epitaxy [5].

Table 1 gives a brief listing and explanation of some terms associated with epitaxy. The process itself is influenced by a range of kinetic and energetic factors that determine the resultant structure. Kinetic considerations in epitaxial growth arise from those processes that require an energy barrier of some sort to be surmounted to allow the growth to proceed. They include dissociation (if the adsorbing species is molecular); diffusion across terraces and along atomic step edges; initial nucleation and aggregation of small clusters; and diffusion along edges of small islands. If any one of the 'kinetic barriers' to these processes is not overcome, this can lead to an intermediate or 'metastable' structure. Where all of the kinetic barriers are surmounted, the resulting structure is the lowest energy solution, determined purely by considerations of the energetic balance of the chemical interactions between the adsorbing species and the substrate, and between the adsorbing atoms themselves [6].

Kinetic factors have been calculated extensively, particularly for simple cases of gas–surface interactions, using a variety of approximate methods. Several rules of thumb for growth morphology have been developed based on considerations of surface and interface energies, although these terms are difficult to measure or calculate with any degree of accuracy, and vary according to the exposed crystal facet. Density functional theory offers a route to calculation of the lowest energy structures; however, most often this is done 'forensically' to confirm a structure that has been inferred by some experimental method [6].

Our goal in this paper is to review studies of epitaxial growth on a particular type of crystal surface—the quasi-crystal—with a view to identifying the key factors in the information-transfer (epitaxial) process. Quasi-crystals are intermetallic compounds of at least two elements. They are a subset of a class of materials known as complex metallic alloys (CMAs) [7]. The latter are characterized by highly symmetric clusters that decorate their large to 'giant' unit cells. Quasi-crystals represent the limiting case where the unit cell can be regarded as infinite, as they lack translational symmetry. Table 2 lists and provides a brief explanation of some terms associated with quasi-crystals.

Table 2. A brief listing and explanation of some terms associated with quasi-crystals.

quasi-crystal:	a type of crystal that is well ordered but not periodic
approximant:	a periodic crystalline material that is closely related to a quasi-crystal, both in chemical composition and in atomic structure
complex metallic alloy:	a crystalline compound composed of metallic constituents, with a large unit cell, containing up to thousands of atoms and the occurrence of well-defined clusters. Approximants are a subset of complex metallic alloys. Quasi-crystals can also be considered a subset, with a unit cell that is infinitely large
Penrose tiling:	a non-periodic tiling generated by one of three aperiodic sets of prototiles named after Roger Penrose, who investigated these sets in the 1970s
Ammann bars:	in some tilings, it is possible to decorate the prototiles with line segments such that they produce a grid of straight lines extending over the whole tiling. Robert Ammann discovered the appropriate decorations for several tilings, among them the Penrose rhomb tilings, where the separation of the bars forms a Fibonacci sequence
Fibonacci sequence:	an aperiodic sequence of short (S) and long (L) intervals, generated by repeated application of the rule $S \rightarrow L$ and $L \rightarrow LS$. The nth word approximating the sequence is the concatenation of the two previous words, and the ratio of successive word lengths, as well as the ratio of the number of letters L and S, approaches the golden mean $\tau = \frac{1+\sqrt{5}}{2}$ when n becomes large.
white flower (WF):	a term used in scanning tunnelling microscope (STM) images of fivefold surfaces of icosahedral surfaces to denote an equatorially truncated Pseudo–Mackay cluster that has an atom at its centre, predominantly Mn
dark star (DS):	a term used in STM images of fivefold surfaces of icosahedral surfaces to denote a vacancy resulting from the irregular decoration of the inner shell of a pseudo-Mackay cluster

There are a number of reasons to choose quasi-crystals for this purpose. Firstly, quasi-crystals are both chemically and structurally complex and hence offer more possibilities in epitaxy than single-crystal low-index surfaces. Secondly, in contrast to other crystal surfaces where atomic reconstructions can take place to minimize the total energy of the system, the complex structure of quasi-crystals are preserved within the topmost surface layers, i.e. the surface is bulk-terminated [8]. This opens up the possibility to use aperiodic surfaces as templates to study the relationship that exists between structural complexity and physical/chemical properties by transferring the surface structure of quasi-crystals to thin films made of a single element. A pseudomorphic thin film of reduced chemical complexity would enable evaluation of the intrinsic properties associated with aperiodic order. Thirdly, as we shall demonstrate, they exhibit a number of surprises in epitaxial growth that serve to illustrate the role of some of the kinetic and energetic factors referred to above.

Further reasons for choosing quasi-crystals are the major contributions that Alan Mackay made to this field. In his seminal 1982 paper entitled ‘Crystallography and the Penrose pattern’ [9], he demonstrated that a Penrose

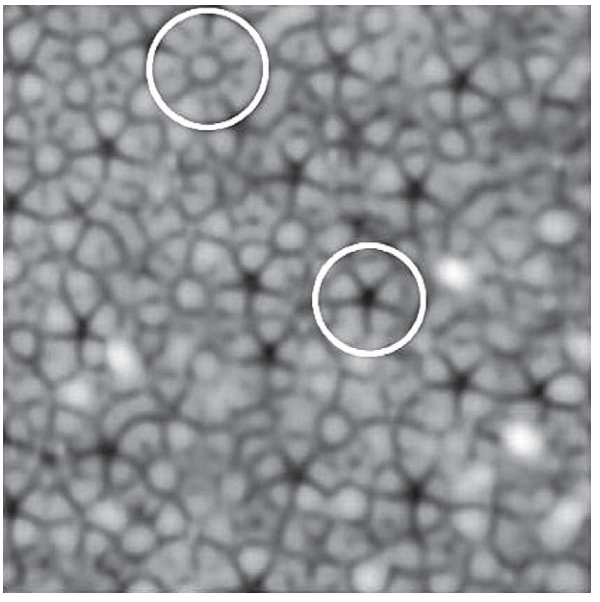

Figure 1. High-resolution STM image (100 × 100 Å) showing the fivefold surface of the icosahedral *i*-Al–Pd–Mn quasi-crystal. The structural motifs known as the white flower (top) and the dark star (middle) are outlined.

tiling [10] has an optical (Fourier) transform which has 10-fold symmetry. He also made the following statement concerning the Penrose tiling:

> It has local five-fold axes and thus represents a structure outside the formalism of classical crystallography and might be designated a quasi-lattice.
>
> [9, p. 609]

His use of the term quasi-lattice anticipated the name 'quasi-crystal' [11] by which the materials discovered by Shechtman and co-workers [12] became known. His name is also associated with one of the two building blocks of the icosahedral F-type quasi-crystals, the pseudo-Mackay cluster [13]. Alan Mackay's contributions to this field are discussed in more detail in a historical review article by Hargittai published in 2010 [14], the same year in which Alan shared the prestigious Oliver E. Buckley Prize of the American Physical Society for his work in this field.

In this paper, we will focus our attention on one particular type of quasi-crystal surface as a substrate—the fivefold surface of icosahedral Al-based quasi-crystals. Scanning tunnelling microscopy (STM) images of the clean surface of icosahedral Al–Pd–Mn (*i*-Al–Pd–Mn) (figure 1) show features such as the white flower (WF)—a truncated pseudo-Mackay cluster which has an underlying Mn atom in its centre, and pentagonal vacancy sites (also known as pentagonal dark stars (DSs)) whose interpretation has been controversial; current thinking favours their interpretation as also being cut pseudo-Mackay clusters, but not cut at the same height as the WFs [15].

The structure of the fivefold surfaces can be interpreted by superimposing aperiodic tilings on models of the surface structure. These can be either Penrose P1 tilings composed of pentagons, fivefold stars, rhombi and boat-shaped tiles or

decagon–hexagon–boat–star (DHBS) tilings consisting of decagons (D), squashed hexagons (H), boats (B) and stars (S) [16]. These tilings are intimately linked and share common vertices; the inter-connection of the centre of the D tiles leads to a τP1 tiling, i.e. the Penrose P1 tiling inflated by $\tau(=1.618\ldots)$. The D tile centres and *a fortiori* the τP1 tiling vertices coincide with the centres of the WFs.

The paper will be organized as follows. We consider examples of epitaxial growth on quasi-crystals in three regimes: sub-monolayer (sub-ML) up to ML; multi-layer; and thin film. This is followed by a discussion and some conclusions.

2. Growth up to a monolayer: Al, Si and Pb on *i*-Al–Pd–Mn

The adsorption of Si atoms on the fivefold surface of the icosahedral *i*-Al–Pd–Mn quasi-crystal serves as a first example. For the sub-ML regime, the Si adatoms are found to self-organize on the surface into an ordered quasi-periodic array [17]. This aperiodic arrangement is confirmed by the 10-fold symmetry of the fast Fourier transform (FFT) calculated from Si atoms distributed across terraces (not shown). An alternative way to visualize this quasi-periodic ordering is shown in figure 2*a*, where the adsorbates are bisected by Ammann bars. The presence of Ammann bars is often taken as a representation of a one-dimensional quasi-periodic structure [18]. The values of the spacing between the lines drawn on figure 2*a* are in agreement with those measured between the pentagonal DSs [19] present on the surface prior to deposition (discussed in §1). Using atomically resolved STM images, a careful inspection of the motifs surrounding the adsorbates coupled with an analysis based on two-dimensional auto-correlation functions pointed to a preferential nucleation site for Si atoms at low coverage. It corresponds to the centre of a truncated *pseudo*-Mackay cluster (one of the basic building blocks of the bulk structure) present at the *i*-Al–Pd–Mn surface—the so-called WFs [13].

For the initial stage of deposition, the adatoms are sufficiently mobile across the surface to find these trapping sites and adsorb. The higher binding energy (deeper potential well) experienced by an Si atom at these sites could result from the presence of a charge density maximum and/or from the tendency to form directional covalent bonds at this precise location. Above a critical dose (0.25 ML), the formation of small Si clusters leads to a disordered film, as confirmed by diffraction techniques [17]. This coverage corresponds to a point where all initial adsorption sites on the template have been decorated. Therefore, above a certain coverage, information on the quasi-periodic order of the substrate is simply lost.

The adsorption of Al atoms on the fivefold surface of *i*-Al–Cu–Fe quasi-crystal, also leads to nucleation [20]. Indeed, the density of the deposited Al islands is independent of the deposition flux used, which suggests nucleation at a specific type of surface site with fixed density. The *i*-Al–Cu–Fe system, isostructural to the *i*-Al–Pd–Mn quasi-crystal, exhibits a bulk-terminated surface [21] with the presence of DS and WF motifs [22]. In contrast to the previous study, the adsorbates do not decorate the WF sites at the early stage of the deposition. As shown in figure 3, the formation of pentagonal islands (resembling starfish) of uniform lateral size, mono-atomic height and identical orientations are observed across almost all terraces. Several of these nano-islands remain incomplete at low coverage (0.04 ML).

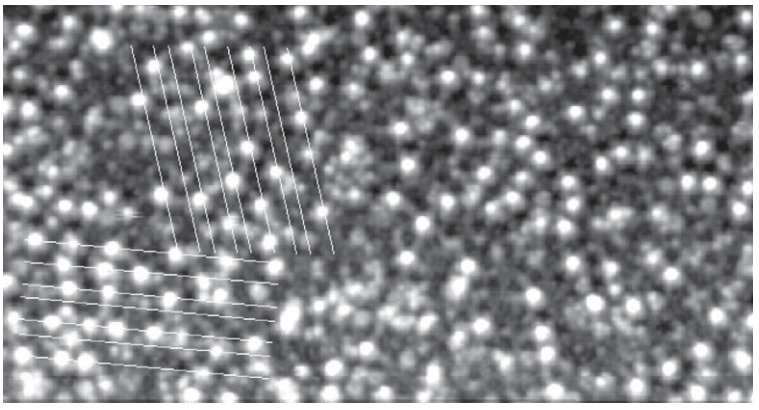

Figure 2. High-resolution STM image (403 × 218 Å) showing the fivefold surface of the icosahedral Al–Pd–Mn quasi-crystal after deposition of 0.25 ML of Si atoms. The adatoms (bright protrusions) are quasi-periodically distributed across the surface. For illustration purposes, two sets of Ammann bars bisecting the adsorbates have been superimposed on the STM image. Reproduced with permission from Ledieu *et al.* [17]. Copyright © APS 2006.

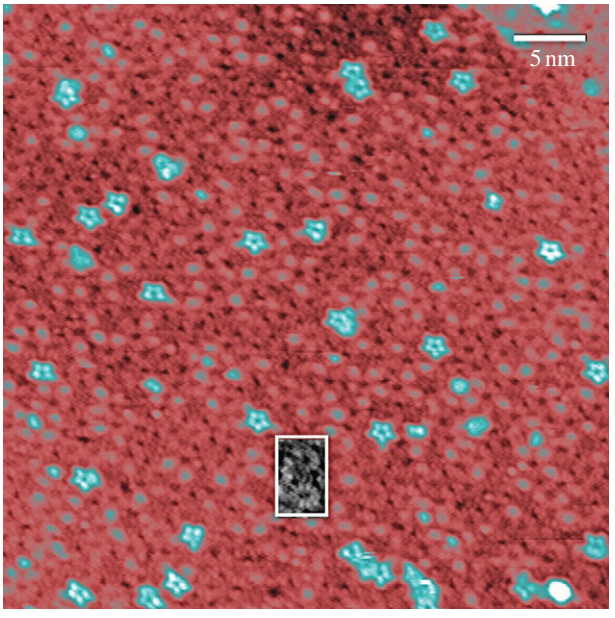

Figure 3. High-resolution STM image (450 × 450 Å) obtained on the fivefold surface of the *i*-Al–Cu–Fe quasi-crystal after deposition of 0.04 ML of Al atoms. The inset shows the underlying substrate. Reproduced with permission from Cai *et al.* [21]. Copyright © Elsevier 2002. (Online version in colour.)

To identify the nucleation site, the starfish positions were analysed with respect to the underlying substrate motifs distinguishable on the STM images. In addition, a thorough analysis of recurrent fivefold atomic arrangements was

carried out for bulk planes that could appear potentially at the alloy topmost surface. Following these detailed measurements and bulk model inspections, the pentagonal surface vacancies or DS sites emerged as the best candidates for the extrinsic Al atoms. To explain the growth mode observed, the nucleation model involves the population of these 2.0 Å deep sites as a prerequisite to the formation of the starfish. First, the Al adatoms diffuse relatively easily across the terraces until they drop into the surface vacancies where they are captured. Then, these trapped adatoms act as nucleation sites for five additional extrinsic Al atoms. If one examines carefully the bulk model, it appears that the adatoms occupy almost the position that would be filled by Al atoms in the upper layer. Hence, not only does this pseudomorphic growth mode result in a quasi-periodic distribution of the starfish, but it replicates local atomic arrangements present within the bulk structure. As demonstrated by Ghosh *et al.* [23], the formation of these starfish can be well understood and reproduced using potential energy surface analysis and kinetic Monte Carlo simulation of a disordered-bond network lattice gas model.

The scenario proposed here is also compatible with the growth mode observed across several terraces where large Al islands are formed at the expense of individual pentagonal nano-islands (see fig. 15 in Fournée & Thiel [24]). A lack of empty DS sites on specific surface planes is theoretically expected and accounts for the growth mode discrepancy observed among terraces. In the absence of such deep potential energy wells, the adsorbate–adsorbate interaction should prevail over the adsorbate–substrate interaction, leading to the lateral growth of dense Al islands and a loss of the aperiodic information. The mobile impinging additional adatoms diffuse across the surface to eventually nucleate at the island step edges. In contrast, the six-atom islands do not grow laterally. This leads to an early roughening of the deposited film.

Both the studies mentioned above lead rapidly to a disordered structure with increasing coverage, so that aperiodic order in the growing layer is lost before the completion of a ML. In contrast, the heterogeneous nucleation of Pb atoms on the fivefold surface of *i*-Al–Pd–Mn results in a well-organized ML. At low coverage, Pb adatoms remain mobile on the surface and diffuse across terraces to self-assemble into pentagonal clusters that display the same monoatomic height, orientation and lateral size on all terraces (figure 4*a*). The formation of these clusters is highly reproducible for different fluxes and over a large sample temperature range (57–653 K). A combination of experimental measurements and *ab initio* calculations was used to identify the precise nucleation site, and to determine the adatom configuration and the number of Pb atoms involved per starfish [25]. The best agreement was obtained for a pentagonal cluster consisting of 10 Pb adatoms arranged as two concentric pentagons pointing in the same direction and located within the decagon tiles, i.e. on top of the WF site. This Pb_{10} atom cluster, shown in figure 4*b*, has the lowest energy configuration that has been found among the several models tested. The comparison between experimental and simulated STM images (figure 4*a*, *c*) is satisfactory, with the main characteristic features (lateral extension, height difference within the clusters) being reproduced. While the adatoms of the central pentagons occupy bridge positions, the five Pb atoms belonging to the outer pentagon nucleate precisely at the centre of small Al pentagons. These sites, corresponding to the vertices of the P1 tiling, are associated with charge density minima on the clean *i*-Al–Pd–Mn surface.

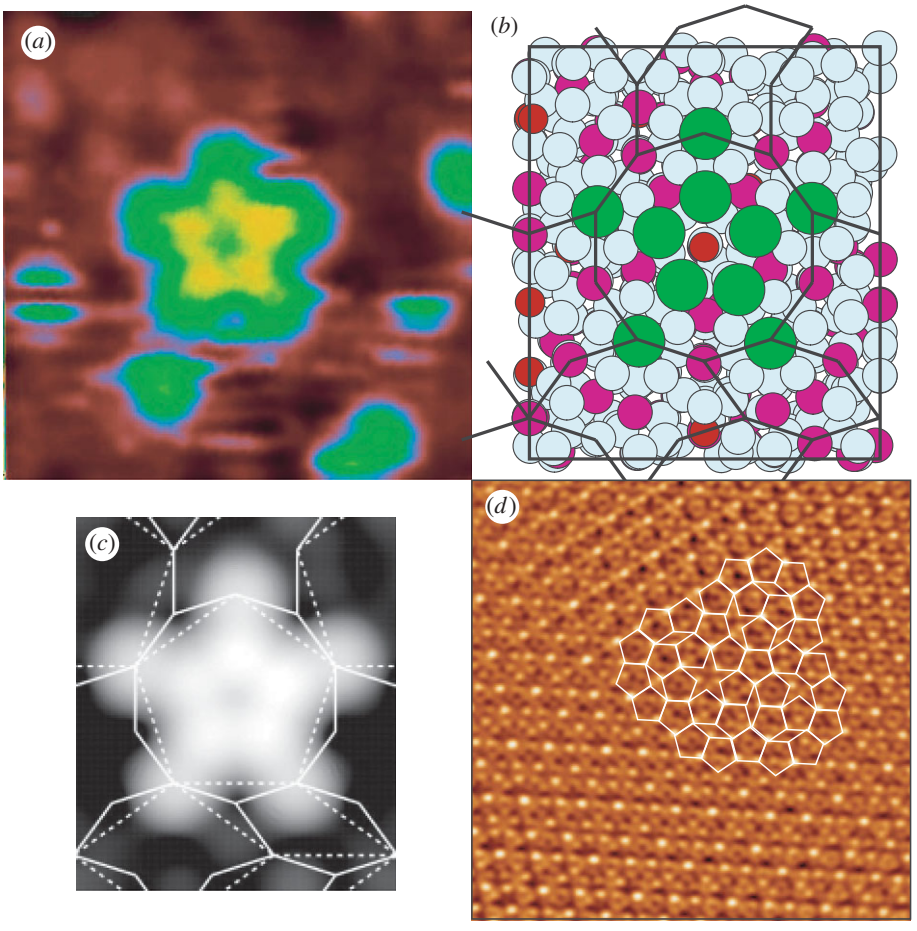

Figure 4. (*a*) Atomically resolved STM (40 × 40 Å) image showing an individual starfish cluster. (*b*) 40 × 40 Å representation of the Pb_{10} atom cluster configuration positioned within the decagon tile of the DHBS tiling (see text). The largest dark (green), the small pale (cyan), the dark (magenta) and the smallest dark (red) spheres represent Pb, Al, Pd and Mn atoms, respectively. (*c*) Simulated STM image (40 × 40 Å) corresponding to the model shown in (*b*), with DBHS (solid line) and Penrose tiling (dotted line) superimposed. (*d*) 250 × 250 Å STM image of 1.0 ML of Pb adsorbed on the *i*-Al–Pd–Mn surface. A τP1 tiling has been superimposed to describe the film structure. Adapted from Ledieu *et al.* [26] and Krajčí *et al.* [27]. Copyright © APS 2008 and APS 2010. (Online version in colour.)

Owing to their planar distribution and their density on the surface termination, a preferential decoration of only the P1 tiling vertices sites would lead to a quasi-periodic overlayer, albeit not dense. However *in situ* measurements demonstrated that Pb atoms can depart from these sites and additional adsorbates are thus required to stabilize the 10-atom cluster. The attractive adsorbate–adsorbate interaction is also evident in the cluster calculations, which demonstrates that the Pb inner pentagon alone is unstable. The presence of the outer pentagons is mandatory for cluster formation. Upon relaxation, the distance between the inner and outer Pb atoms becomes close to the nearest-neighbour distance in face-centred-cubic (fcc) Pb [25].

With increasing deposition, other sites present across the surface are populated until the density of the film reaches ≈0.09 atom $Å^{-2}$.The STM image shown in figure 4*d* corresponds to such a coverage of Pb. The roughness and the overall perfection of the ML are improved if dosing is performed while holding the sample at 653 K. The τP1 tiling is used to describe the aperiodic ordering of the Pb ML as it corresponds to the smallest recognizable tiling with the resolution obtained for this coverage. This pseudomorphic thin film can be regarded as an inflated version ($\times\tau$) of the P1 tiling of the clean surface [19,28]. The tiling has been built so as to maximize the coincidence between τP1 vertices with features of highest contrast. The contrast variation observed across the film can be explained using the results of the *ab initio* calculations. Some bright features may result from protruding Pb atoms that sit slightly above their neighbours in this structurally complex ML. Others originate from the adlayer–substrate structural relaxation. Depending on the bond strength with the surrounding atoms, some specific Al atoms can indeed be lifted above the surface plane, hence pushing up the adsorbate above its neighbours. The *ab initio* calculations also indicate a large corrugation of the Pb film, a consequence of the disparate strength of the adsorbate–substrate bonds resulting from the adsorption of Pb within surface vacancies, at hollow sites and at bridge positions [27].

3. Beyond a monolayer: growth of Bi islands on quasi-crystal surfaces

Growth of Pb on *i*-Al–Pd–Mn saturates at ML coverage. To explore what happens in growth on quasi-crystals above this coverage, we turn to another adsorbate, Bi. Growth of Bi on the surfaces of quasi-crystals has been intensively studied because of the rich variety of structures that result. Table 3 summarizes experimental studies of Bi growth on various fivefold icosahedral quasi-crystal surfaces reported to date. The growth of the Bi ML was first reported by Franke *et al.* [29]. In experiments using helium atom scattering (HAS) and low-energy electron diffraction (LEED), it was found that Bi forms a quasi-crystalline ML when deposited on the fivefold surface of *i*-Al–Pd–Mn or on the 10-fold surface of decagonal (*d*)-Al–Ni–Co [29]. HAS provides exclusive information of the topmost layer. Both HAS and LEED from the ML show the same symmetry and peak positions as those from the respective clean surfaces, evidencing the quasi-crystalline structure of the ML. The stability of this ML was later supported by *ab initio* calculations [16,35] and other experimental techniques such as STM [31] and medium-energy ion scattering (MEIS) [33].

The nucleation and growth of the pseudomorphic ML on the *i*-Al–Pd–Mn surface were studied using STM, and follow a similar pattern to that for Pb on the same surface, with nucleation of pentagonal clusters at pseudo-Mackay adsorption sites [31]. These nucleation sites are quasi-periodically distributed and their density is about half of a ML. The subsequent deposition of Bi completes the ML.

In the first report of the Bi ML [29], Bi was deposited at an elevated substrate temperature of about 300°C, which was above the multi-layer desorption temperature, so that only the ML could be adsorbed. Sharma *et al.* later performed experiments at room temperature and identified the formation of crystalline islands after the completion of the quasi-crystalline

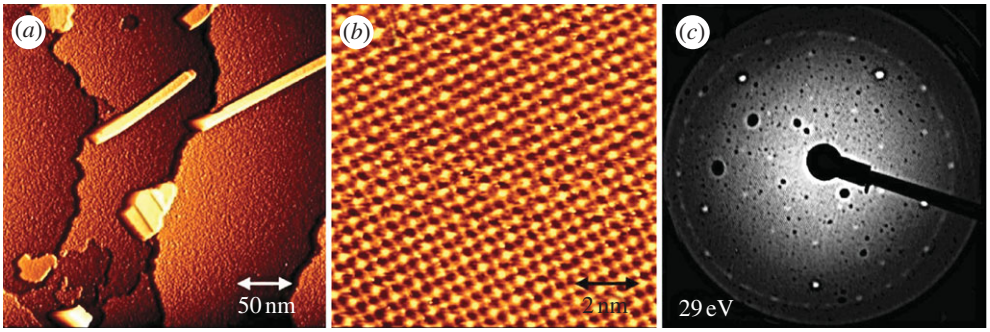

Figure 5. (*a*,*b*) STM images of the fivefold *i*-Al–Pd–Mn surface after deposition of Bi, showing the Bi pseudo-cubic islands (bright areas) (*a*, coverage: 1.8 MLE) and atomic structure of a pseudo-cubic island (*b*, coverage 4.1 MLE). (*c*) LEED pattern from the Bi pseudo-cubic allotrope (coverage 4.1 MLE). The black dots are an instrumental artefact. Adapted from Smerdon *et al.* [32]. Copyright © IOP 2010. (Online version in colour.)

Table 3. A list of experimental studies on Bi thin-film growth on icosahedral fivefold quasi-crystal surfaces (HAS, helium atom scattering, LEED, low-energy electron diffraction, RHEED, reflection high-energy electron diffraction, STM, scanning tunnelling microscopy, XPS, X-ray photoemission spectroscopy, MEIS, medium-energy ion scattering).

substrate	method	authors	reference	observation
i-Al–Pd–Mn	HAS, LEED	Franke *et al.*	[29]	quasi-crystalline monolayer
i-Al–Cu–Fe	STM, RHEED	Fournée *et al.*	[24]	magic height islands
i-Al–Pd–Mn	STM	Sharma *et al.*	[30]	magic height islands
i-Al–Cu–Fe	STM	Sharma *et al.*	[30]	magic height islands
i-Al–Pd–Mn	STM	Smerdon *et al.*	[31]	structure of monolayer
i-Al–Pd–Mn	STM	Smerdon *et al.*	[32]	structure of islands
i-Al–Pd–Mn	MEIS	Noakes *et al.*	[33]	structure of monolayer and islands
i-Al–Pd–Mn	XPS	Young *et al.*	[34]	stability of monolayer and islands

ML on *i*-Al–Pd–Mn, as well as on *i*-Al–Cu–Fe and *d*-Al–Ni–Co [24,30]. A recent quantitative analysis by X-ray photoemission spectroscopy (XPS) of Bi/*i*-Al–Pd–Mn has confirmed the growth and the stability of the islands [34].

The Bi islands exhibit specific heights (the so-called 'magic heights'), which correspond to the stacking of four atomic layers (4L) or multiples of this height [24,30,32,33,36] (figure 5*a*). Here, coverage is quoted in units of monolayer equivalent (MLE), where the calibration is fixed by the deposition of the first ML. Islands of two atomic heights were also observed at an early stage of the growth. However, these islands either reshaped themselves into 4L islands or they coalesce with neighbouring 4L islands [30].

The distribution of the island heights on *d*-Al–Ni–Co was found to be dependent on substrate temperature and deposition flux. High flux or low substrate temperature yield islands of uniform height of 4L [36]. The observation of the magic heights is believed to be due to quantum size effects [24]. The

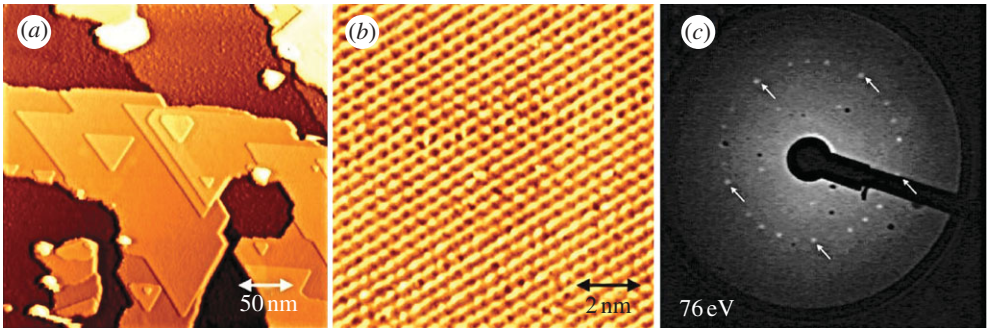

Figure 6. (*a*,*b*) STM images of the fivefold *i*-Al–Pd–Mn surface after deposition of Bi, showing (*a*) the Bi hexagonal islands and (*b*) atomic structure of a hexagonal island surface. (*c*) LEED pattern from the Bi hexagonal allotrope (coverage 4.1 MLE). The arrows indicate the high-symmetry spots of the substrate. Adapted from Smerdon *et al.* [32]. Copyright © IOP 2010. (Online version in colour.)

substrate–film and film–vacuum interfaces act as a confinement barrier, such that electrons travelling perpendicular to the surface reflect from the interfaces, which results in quantum well states. The thickness of the islands is then influenced by the position of the quantum well states. Magic heights have been also observed in Ag films grown on *i*-Al–Pb–Mn [24,37]. The electron confinement was originally explained in terms of the pseudo-gap in electronic density of states at the Fermi level of the substrate, i.e. if the energy of the Bi or Ag *sp* electrons, which dominate the valence bands of these metals, lies in the pseudo-gap of the substrate, the electrons are reflected at the interface [24]. This interpretation was later disputed by a photoemission study on Ag/*i*-Al–Pd–Mn. It was argued instead that the confinement arises from incompatible symmetries of electronic states in the quasi-crystalline substrate and crystalline film such that no coupling of electron wave functions occurs at the interface [37].

These islands have pseudo-cubic structure with the {100} surface orientation. This structure was initially revealed by STM and reflection high-energy electron diffraction (RHEED) from Bi/*i*-Al–Cu–Fe [24] and recently confirmed by MEIS [33] from Bi/*i*-Al–Pd–Mn. Figure 5*b* shows the atomic structure expected for a pseudo-cubic {100} island. The MEIS results reveal the formation of bilayers within the islands, resembling a distorted black-phosphorous structure [33]. LEED indicates that the islands are randomly aligned with the substrate; such a random distribution of the islands yields a diffuse ring in the LEED pattern. (figure 5*c*) [32].

Above a critical coverage, the pseudo-cubic {100} islands transform to the hexagonal {0001} surface orientation (figure 6*a*) [32,36], which is the natural cleavage plane of bulk Bi [38]. The triangular symmetry of the islands, as well as the hexagonal unit cell observed in STM (figure 6*b*), is indicative of this structure. The hexagonal structure is also confirmed by LEED. Unlike the pseudo-cubic islands, the hexagonal islands maintain an orientational relationship with the substrate. LEED from the system provides 30 spots, arising from hexagonal domains aligned along the five high-symmetry directions of the

substrate (figure 6*c*) [32]. The position of the spots are consistent with those expected for the hexagonal structure and also coincides with the Bragg peaks of the substrate, which establishes the film–substrate registry.

4. Fibonacci film formation: Cu adsorption on *i*-Al–Pd–Mn

Most of the systems that show a degree of transference of structural information from the quasi-crystalline substrate to an adsorbate are those in which the adsorbate is a metal with a large atomic radius and a low melting point [29–32]. When transition metals are used as an adsorbate, in some cases, rotational epitaxy is the resultant growth mode [39,40]. In this growth mode, the only information transferred is the degree of rotational symmetry of the substrate. That is, a fivefold substrate will lead to the growth of crystalline domains with no relation to the substrate other than that one crystal direction of the growing film will be coincident with a high-symmetry direction of the quasi-crystalline substrate.

Cobalt, when deposited on *d*-Al–Ni–Co and, in particular, Cu, when deposited on *i*-Al–Pd–Mn, show some rather different behaviour, which is intermediate to the two cases referred to above [41–44]. STM images of the structure of 4 ML of Cu/*i*-Al–Pd–Mn show the formation of a 'stripe' pattern at the surface of the film. For each domain, the stripe pattern runs in one direction only; the observation of five stripe patterns leads to the conclusion that the film comprises nanocrystallites of five orientational domains, as may be expected on a fivefold surface. These structures are shown in figure 7.

The stripe pattern is an emergent phenomenon and is not visible at lower coverages. The film appears disordered and unresolved at coverages under a ML. Between 1 and 3 ML, some ordering becomes apparent in the straightening of island edges, and certain pentagonal directions become apparent between domains. The stripe pattern itself appears after around 3 ML, and can be described as a set of Ammann bars where the sequence of separations is equivalent to a one-dimensional Fibonacci chain denoted by stripes of two characteristic widths that are related to each other by τ, the 'golden ratio'. Such a Fibonacci chain may be drawn on images of the clean *i*-Al–Pd–Mn surface simply by joining up like features in the images, such as the truncated pseudo-Mackay clusters (WFs) [45].

The film is very well ordered, as evidenced by high-quality LEED patterns and STM images. It also persists to at least 25 ML with the same structure, though it becomes increasingly three dimensional with increasing coverage. A simple analysis of the LEED pattern, reproduced in figure 8 [42], identified the characteristic 'streaking' in the patterns as due to the Fibonacci chain of streak separations present at the film surface. As the streaks are due to the Fibonacci ordering, the *separation* of the streaks must be related to the lattice parameter in the real-space direction *perpendicular* to the stripe pattern. This allowed for the extraction of a surface unit cell parameter of around 2.5 Å, compatible with an fcc (100) orientation, and thus presenting a plausible simple model for the film structure. When MEIS data were collected from this film [43], this model of the film structure was used as the starting point for the Monte Carlo analysis of the blocking dips in the spectra, and ultimately yielded a good fit to the experimental

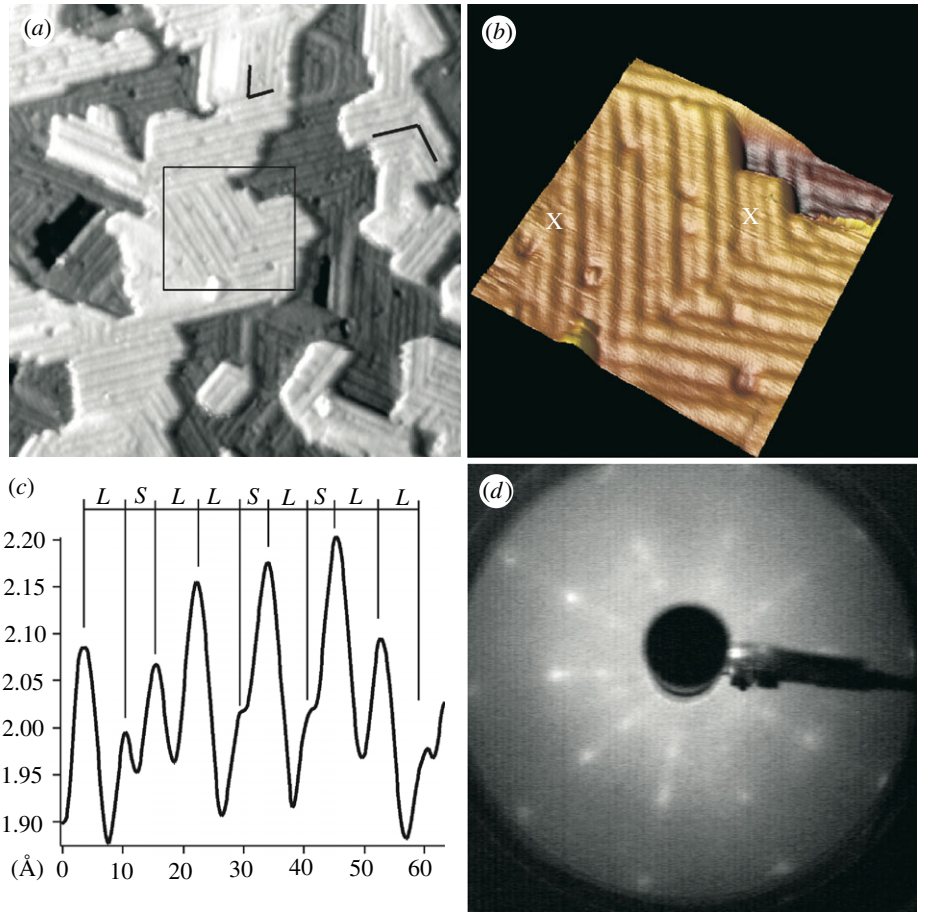

Figure 7. (*a*) 400 × 400 Å STM image of the fivefold surface of *i*-Al–Pd–Mn after deposition of 5.5 ML of Cu. (*b*) 100 × 100 Å detail from (*a*). (*c*) A profile between the points marked with a cross in (*b*); it demonstrates that the sequence of Cu rows is quasi-periodic with spacings given by *LSLLSLSLL*, where $S = 4.5 \pm 0.2$ Å and $L = 7.3 \pm 0.3$ Å. The ratio of these numbers equals the golden mean τ within experimental error. (*d*) LEED pattern (beam energy 50 eV) corresponding to this phase. The relationships between spot positions are indicative of τ-scaling. See also the LEED pattern from this system at 335 eV in figure 8. Adapted from Ledieu *et al.* [41]. Copyright © APS 2004. (Online version in colour.)

data. The specific characteristics of the model thus generated can be summarized in the following manner: five domains of a crystalline fcc [100] Cu structure, oriented at pentagonal angles to each other, with long and short separations comprising two or three atomic planes of Cu stabilized in a strain-based structure.

This conclusion was not supported by some of the experimental observations, however. First of all, there is no clear reason why stripes would be visible *at all* if there were not also some associated variations in topography. Secondly, it seems unlikely that such a structure could be stable at coverages reaching 25 ML. Thirdly, it follows that for a strain-based structure, the stripe pattern would be most visible in the first layer where the substrate influence is at a maximum.

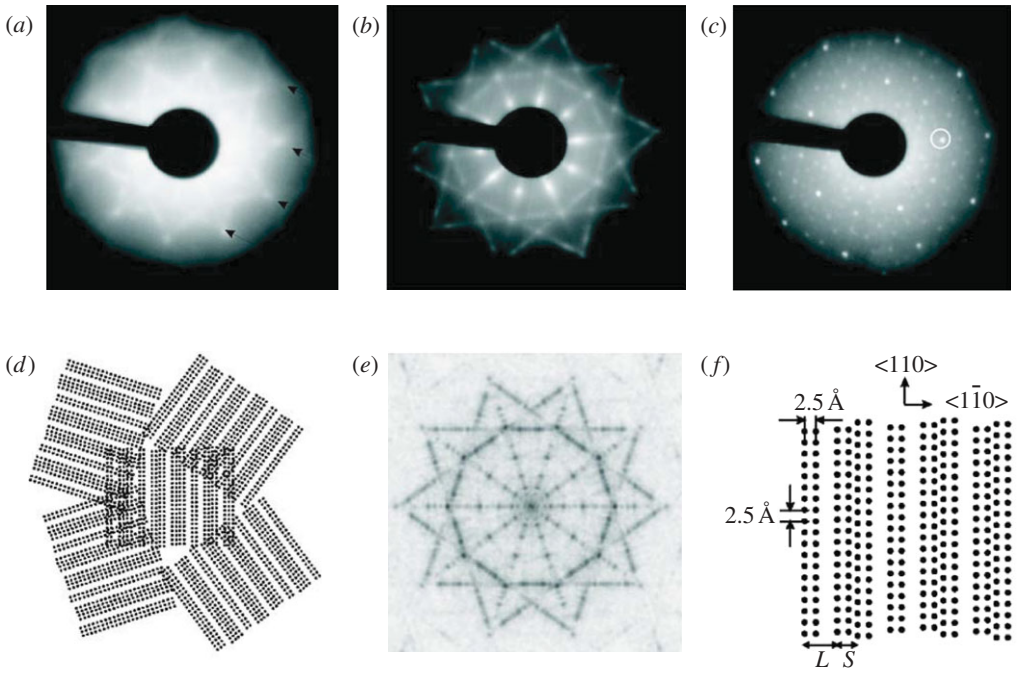

Figure 8. (*a*) LEED pattern from the Cu film on *i*-Al–Pd–Mn at 335 eV. The surface temperature was 85 K. The arrows indicate the locations of periodically spaced streaks in the diffraction pattern. The streaks are present in five directions, separated by 72° (see also the LEED pattern in (*b*)). (*b*) LEED pattern from the same surface at 169 eV. At this energy, only the zeroth-order and first-order streaks are apparent. (*c*) LEED pattern from the clean *i*-Al–Pd–Mn surface at 169 eV. The circled spot indicates the (32002) spot indexed in Schaub *et al.* [46]. (*d*) Model structure: five domains of the model structure shown in (*f*). (*e*) Fourier transform of the model structure. (*f*) A single domain of the model structure. Adapted from Ledieu *et al.* [42]. Copyright © APS 2005. (Online version in colour.)

Because of these problems, a dynamical LEED analysis of the structure [47] was carried out. This analysis yielded a model that addressed all of the problems in the strain-based model and explained all of the experimental observations. This model, shown in figure 9, is based on a body-centred tetragonal (bct) lattice with an associated rotation leaving the *ab* plane at an angle of 13.28° to the substrate surface plane. This rotation provides a one-dimensional pattern of steps at the Cu/*i*-Al–Pd–Mn interface with an approximately Fibonacci character that mirrors the separations of certain points of high symmetry in the substrate surface. This pattern of steps is reproduced at the surface of the Cu film and gives rise to the stripe pattern. Such a structure has very little inherent strain, accounting for its stability at higher film thicknesses. Also, the unit cell of such a three-dimensional superstructure would contain much more material than a comparable unit cell for the two-dimensional class of superstructures, which explains why the stripe pattern is not visible at low coverages.

The original account of this film reported that the film growth followed the Stranski–Krastanov model. The standard interpretation of Stranski–Krastanov style growth is that a pseudomorphic wetting layer is formed of indeterminate

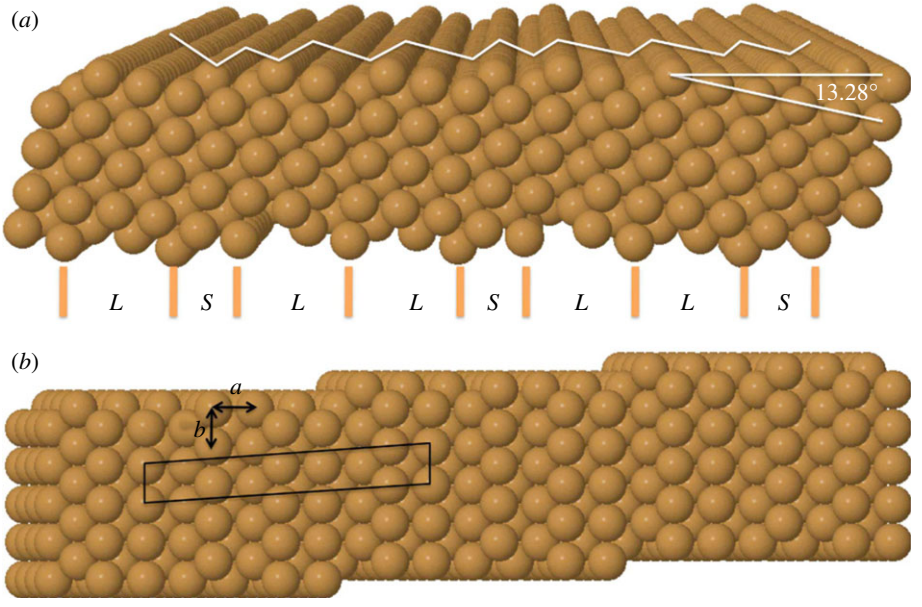

Figure 9. (*a*) Perspective side view of the vicinal body-centred orthorhombic *LSL* model, showing the *L* and *S* distances across the bottom and a schematic of the step structure at the top. (*b*) Top view of the stepped same model, showing the surface unit cell. Adapted from Pussi *et al.* [47]. Copyright © IOP 2009. (Online version in colour.)

but low thickness, followed by nucleation of islands of a normal crystalline form of the adsorbate. This is clearly not what is happening for this film, which is more like Volmer–Weber (layer-by-layer) style growth in that the adsorbate fails to revert to standard bulklike Cu for any thickness up to at least 25 ML.

5. Discussion and conclusions

As demonstrated by the examples above, adsorbate–substrate and adsorbate–adsorbate interactions play a crucial role in information-transferring epitaxial processes on quasi-crystal surfaces. Only heterogeneous nucleation has been found to lead to the pseudomorphic growth of MLs. Additionally, of the two adsorption sites identified on the fivefold *i*-Al–Pd–Mn surface—the DS and WF—only decoration of the WFs results in dense aperiodic MLs. The degree of ordering is dictated by the local adsorbate–adsorbate interaction, the size of the adsorbates and how they can be accommodated within the P1 or DHBS tilings [48]. Above an ML, Bi adsorbs, but its structure reverts to islands with the structure of bulk Bi allotropes. Initially, pseudo-cubic islands with the (100) surface orientation are formed, which have specific magic heights. This effect is believed to be due to the confinement of electrons within the islands. Above a critical coverage, the overlayer adopts a new morphology with the hexagonal {0001} surface orientation. The hexagonal islands are aligned along the high-symmetry directions of the

substrate, yielding a fivefold-twinned structure. For the case of the Cu film, a unique structure is formed that is heavily influenced by the substrate and persists to many atomic layer thicknesses.

The examples above illustrate the difficulties in information transfer via epitaxy for quasi-crystal surfaces. The situation may improve as new quasi-crystals are discovered and their surfaces in turn are used for epitaxy [49,50]. Another promising area is the use of quasi-crystal surfaces and quasi-periodic overlayers as templates for molecular quasi-crystals [51]. In fact, although quasi-crystal surfaces are chemically and structurally complex, many of the above-mentioned conclusions are valid for all crystal surfaces. While some general principles have been established, attempting to predict what will happen during epitaxial processes is difficult. In many cases, it is not even possible to successfully model experimentally determined structures with the best theoretical tools available.

One can also speculate on the wider question of whether self-organization in epitaxial processes can be a realistic mechanism for information replication. In terms of structural perfection in overlayers and nanostuctures, with a few notable exceptions in semiconductor systems, epitaxial structures are far from achieving the levels of reproducibility and perfection required in industrial manufacturing processes. For example, Motorola and many other companies operate a Six Sigma strategy; a Six Sigma process being one in which 99.99966 per cent of the products manufactured are statistically expected to be free of defects (3.4 defects per million) [52]. It is doubtful whether epitaxy or any other nanoscale self-organization process for construction/replication will ever achieve such a level of perfection, owing to the large number of kinetic and energetic factors that are inherent in such complex processes.

R.McG. thanks the EPSRC for part-funding this project under grant EP/D071828/1. H.R.S. is grateful to the Physical Sciences Research Council for financial support (grant no. EP/D05253X/1). J.L. thanks the Agence Nationale de la Recherche, reference ANR- 08-Blan-0041-01, for its financial support.

References

1 Vishveshwara, S. 2012 A glimpse of quantum phenomena in optical lattices. *Phil. Trans. R. Soc. A* **370**, 2916–2929. (doi:10.1098/rsta.2011.0248)
2 Travers, A. A., Muskhelishvili, G. & Thompson, J. M. T. 2012 DNA information: from digital code to analogue structure. *Phil. Trans. R. Soc. A* **370**, 2960–2986. (doi:10.1098/rsta.2011.0231)
3 McGlynn, S. E., Kanik, I. & Russell, M. J. 2012 Peptide and RNA contributions to iron–sulphur chemical gardens as life's first inorganic compartments, catalysts, capacitors and condensers. *Phil. Trans. R. Soc. A* **370**, 3007–3022. (doi:10.1098/rsta.2011.0211)
4 Cademartiri, L., Bishop, K. J. M., Snyder, P. W. & Ozin, G. A. 2012 Using shape for self-assembly. *Phil. Trans. R. Soc. A* **370**, 2824–2847. (doi:10.1098/rsta.2011.0254)
5 Brune, H. 1998 Microscopic view of epitaxial metal growth: nucleation and aggregation. *Surf. Sci. Rep.* **31**, 121–229. (doi:10.1016/s0167-5729(99)80001-6)
6 Zangwill, A. 1988 *Physics at surfaces*. Cambridge, UK: Cambridge University Press.
7 Dubois, J.-M. & Belin-Ferré, E. 2011 *Complex metallic alloys*. Weinheim, Germany: Wiley.
8 Sharma, H. R., Shimoda, M. & Tsai, A. P. 2007 Quasicrystal surfaces: structure and growth of atomic overlayers. *Adv. Phys.* **56**, 403–464. (doi:10.1080/00018730701269773)
9 Mackay, A. L. 1982 Crystallography and the Penrose pattern. *Physica* **114A**, 609–613. (doi:10.1016/0378-4371(82)90359-4)

10 Penrose, R. 1974 The rôle of aesthetics in pure and applied mathematical research. *Bull. Inst. Math. Appl.* **10**, 266.
11 Levine, D. & Steinhardt, P. J. 1984 Quasicrystals: a new class of ordered structures. *Phys. Rev. Lett.* **53**, 2477–2480. (doi:10.1103/PhysRevLett.53.2477)
12 Shechtman, D., Blech, I., Gratias, D. & Cahn, J. W. 1984 Metallic phase with long-range orientational order and no translational symmetry. *Phys. Rev. Lett.* **53**, 1951–1953. (doi:10.1103/PhysRevLett.53.1951)
13 Gratias, D., Puyraimond, F., Quiquandon, M. & Katz, A. 2000 Atomic clusters in icosahedral F-type quasicrystals. *Phys. Rev. B* **63**, 024202. (doi:10.1103/PhysRevB.63.024202)
14 Hargittai, I. 2010 Structures beyond crystals. *J. Mol. Struct.* **976**, 81–86. (doi:10.1016/j.molstruc.2010.02.009)
15 Krajčí, M. & Hafner, J. 2006 Ab-initio study of a quasiperiodic Bi monolayer on a fivefold icosahedral Al-Pd-Mn surface. *Philos. Magn* **86**, 825–830. (doi:10.1080/14786430500256334)
16 Krajčí, M. & Hafner, J. 2005 *Ab initio* study of quasiperiodic monolayers on a fivefold i-AlPdMn surface. *Phys. Rev. B* **71**, 184207. (doi:10.1103/PhysRevB.71.184207)
17 Ledieu, J., Unsworth, P., Lograsso, T. A., Ross, A. R. & McGrath, R. 2006 Ordering of Si atoms on the fivefold Al-Pd-Mn quasicrystal surface. *Phys. Rev. B* **73**, 012204. (doi:10.1103/PhysRevB.73.012204)
18 Schaub, T. M., Bürgler, D. E., Güntherodt, H. J. & Suck, J. B. 1994 Quasicrystalline structure of icosahedral $Al_{68}Pd_{23}Mn_9$ resolved by scanning tunneling microscopy. *Phys. Rev. Lett.* **73**, 1255–1258. (doi:10.1103/PhysRevLett.73.1255)
19 Papadopolos, Z., Kasner, G., Ledieu, J., Cox, E. J., Richardson, N. V., Chen, Q., Diehl, R. D., Lograsso, T. A., Ross, A. R. & McGrath, R. 2002 Bulk termination of the quasicrystalline five-fold surface of $Al_{70}Pd_{21}Mn_9$. *Phys. Rev. B* **66**, 184207. (doi:10.1103/PhysRevB.66.184207)
20 Cai, T., Ledieu, J., McGrath, R., Fournée, V., Lograsso, T. A., Ross, A. R. & Thiel, P. A. 2003 Pseudomorphic starfish: nucleation of extrinsic metal atoms on a quasicrystalline substrate. *Surf. Sci.* **526**, 115–120. (doi:10.1016/S0039-6028(02)02593-1)
21 Cai, T., Fournée, V., Ross, A. R., Lograsso, T. A. & Thiel, P. A. 2002 An STM study of the atomic structure of the icosahedral Al-Cu-Fe fivefold surface. *Phys. Rev. B* **65**, 140202. (doi:10.1103/PhysRevB.65.140202)
22 Ledieu, J., Dhanak, V. R., Diehl, R. D., Lograsso, T. A., Delaney, D. W. & McGrath, R. 2002 Sulphur adsorption on the fivefold surface of the *i*-Al–Pd–Mn quasicrystal. *Surf. Sci.* **512**, 77–83. (doi:10.1016/S0039-6028(02)01575-3)
23 Ghosh, C., Liu, D. J., Schnitzenbaumer, K. J., Jenks, C. J., Thiel, P. A. & Evans, J. W. 2006 Island formation during Al deposition on 5-fold Al–Cu–Fe quasicrystalline surfaces: kinetic Monte Carlo simulation of a disordered-bond-network lattice-gas model. *Surf. Sci.* **600**, 2220–2230. (doi:10.1016/j.susc.2006.03.013)
24 Fournée, V. & Thiel, P. A. 2005 New phenomena in epitaxial growth: solid films on quasicrystalline substrates. *J. Phys. D Appl. Phys.* **38**, R83–R106. (doi:10.1088/0022-3727/38/6/R01)
25 Ledieu, J., Krajčí, M., Hafner, J., Leung, L., Wearing, L. H., McGrath, R., Lograsso, T. A., Wu, D. & Fournée, V. 2009 Nucleation of Pb starfish clusters on the five-fold Al-Pd-Mn quasicrystal surface. *Phys. Rev. B* **79**, 165430. (doi:10.1103/PhysRevB.79.165430)
26 Ledieu, J., Leung, L., Wearing, L. H., McGrath, R., Lograsso, T. A., Wu, D. & Fournée, V. 2008 Self-assembly, structure and electronic properties of a quasiperiodic Pb monolayer. *Phys. Rev. B.* **77**, 073409. (doi:10.1103/PhysRevB.77.073409)
27 Krajčí, M., Hafner, J., Ledieu, J., Fournée, V. & McGrath, R. 2010 Quasiperiodic Pb monolayer on the fivefold *i*-Al–Pd–Mn surface: structure and electronic properties. *Phys. Rev. B* **82**, 085417. (doi:10.1103/PhysRevB.82.085417)
28 Ledieu, J., McGrath, R., Diehl, R. D., Lograsso, T. A., Delaney, D. W., Papadopolos, Z. & Kasner, G. 2001 Tiling of the fivefold surface of $Al_{70}Pd_{21}Mn_9$. *Surf. Sci.* **492**, L729–L734. (doi:10.1016/S0039-6028(01)01463-7)
29 Franke, K. J., Sharma, H. R., Theis, W., Gille, P., Ebert, Ph. & Rieder, K. H. 2002 Quasicrystalline epitaxial single element monolayers on icosahedral Al-Pd-Mn and decagonal Al-Ni-Co quasicrystal surfaces. *Phys. Rev. Lett.* **89**, 156104. (doi:10.1103/PhysRevLett.89.156104)

30 Sharma, H. R., Fournée, V., Shimoda, M., Ross, A. R., Lograsso, T. A., Gille, P. & Tsai, A. P. 2008 Growth of Bi thin films on quasicrystal surfaces. *Phys. Rev. B* **78**, 155416. (doi:10.1103/PhysRevB.78.155416)
31 Smerdon, J. A., Parle, J. K., Wearing, L. H., Lograsso, T. A., Ross, A. R. & McGrath, R. 2008 Nucleation and growth of a quasicrystalline monolayer: Bi adsorption on the fivefold surface of *i*-$Al_{70}Pd_{21}Mn_9$. *Phys. Rev. B* **78**, 075407. (doi:10.1103/PhysRevB.78.075407)
32 Smerdon, J. A., Cross, N., Dhanak, V. R., Sharma, H. R., Young, K. M., Lograsso, T. A., Ross, A. R. & McGrath, R. 2010 Structure and reactivity of Bi allotropes on the fivefold icosahedral Al–Pd–Mn quasicrystal surface. *J. Phys., Condens. Matter* **22**, 345002. (doi:10.1088/0953-8984/22/34/345002)
33 Noakes, T. C. Q. *et al.* 2010 Two- and three-dimensional growth of Bi on *i*-Al–Pd–Mn studied using medium energy ion scattering. *Phys. Rev. B* **82**, 195418. (doi:10.1103/PhysRevB.82.195418)
34 Young, K. M., Cross, N., Smerdon, J. A., Dhanak, V. R., Sharma, H. R., Lograsso, T. A., Ross, A. R. & McGrath, R. 2011 XPS study of adsorption and desorption of a Bi thin film on the five-fold icosahedral Al-Pd-Mn surface. *Philos. Magn* **91**, 2889–2893. (doi:10.1080/14786435.2010.536793)
35 Krajčí, M., Hafner, J. & Jahnatek, M. 2006 *Ab initio* study of quasiperiodic Bi monolayers on a tenfold d-Al-Co-Ni surface. *Phys. Rev. B* **73**, 184202. (doi:10.1103/PhysRevB.73.184202)
36 Sharma, H. R., Ledieu, J., Fournée, V. & Gille, P. 2011 Influence of the substrate temperature and deposition flux in the growth of a Bi thin film on the ten-fold decagonal Al-Ni-Co surface. *Philos. Magn* **91**, 2870–2878. (doi:10.1080/14786435.2010.507180)
37 Moras, P., Weisskopf, Y., Longchamp, J.-N., Erbudak, M., Zhou, P. H., Ferrari, L. & Carbone, C. 2006 Quantum size effects arising from incompatible point-group symmetries: angle-resolved photoemission study. *Phys. Rev. B* **74**, 121405(R). (doi:10.1103/PhysRevB.74.121405)
38 Hofmann, P. 2006 The surfaces of bismuth: structural and electronic properties. *Prog. Surf. Sci.* **81**, 191–245. (doi:10.1016/j.progsurf.2006.03.001)
39 Wearing, L. H., Smerdon, J. A., Leung, L., Lograsso, T. A., Ross, A. R. & McGrath, R. 2007 Iron deposition on the five-fold surface of the icosahedral Al–Pd–Mn quasicrystal. *Surf. Sci.* **601**, 3450–3455. (doi:10.1016/j.susc.2007.06.028)
40 Wearing, L. H., Smerdon, J. A., Leung, L., Dhesi, S. S., Ledieu, J., Bencok, P., Fisher, I., Jenks, C. J. & McGrath, R. 2008 Iron deposition on the tenfold surface of the $Al_{72}Ni_{11}Co_{17}$ decagonal quasicrystal. *J. Phys., Condens. Matter* **20**, 015005. (doi:10.1088/0953-8984/20/01/015005)
41 Ledieu, J., Hoeft, J. T., Reid, D. E., Smerdon, J. A., Diehl, R. D., Lograsso, T. A., Ross, A. R. & McGrath, R. 2004 Pseudomorphic growth of a quasiperiodic copper thin film on a quasicrystal surface. *Phys. Rev. Lett.* **92**, 135507. (doi:10.1103/PhysRevLett.92.135507)
42 Ledieu, J., Hoeft, J. T., Reid, D. E., Smerdon, J. A., Diehl, R. D., Ferralis, N., Lograsso, T. A., Ross, A. R. & McGrath, R. 2005 Copper adsorption on the fivefold $Al_{70}Pd_{21}Mn_9$ quasicrystal surface. *Phys. Rev. B* **72**, 035420. (doi:10.1103/PhysRevB.72.035420)
43 Smerdon, J. A., Ledieu, J., McGrath, R., Noakes, T. C. Q., Bailey, P., Drexler, M., McConville, C. F., Lograsso, T. A. & Ross, A. R. 2006 Characterization of aperiodic and periodic thin Cu films formed on the five-fold surface of i-$Al_{70}Pd_{21}Mn_9$ using medium-energy ion scattering spectroscopy. *Phys. Rev. B* **74**, 035429. (doi:10.1103/PhysRevB.74.035429)
44 Smerdon, J. A., Ledieu, J., Hoeft, J. T., Reid, D. E., Wearing, L. H., Diehl, R. D., Lograsso, T. A., Ross, A. R. & McGrath, R. 2006 Adsorption of cobalt on the tenfold surface of $Al_{72}Ni_{11}Co_{17}$ and on the fivefold surface of $Al_{70}Pd_{21}Mn_9$. *Philos. Magn* **86**, 841–848. (doi:10.1080/14786430500263447)
45 Ünal, B., Jenks, C. J. & Thiel, P. A. 2009 Adsorption sites on icosahedral quasicrystal surfaces: dark stars and white flowers. *J. Phys., Condens. Matter* **21**, 055009. (doi:10.1088/0953-8984/21/5/055009)
46 Schaub, T. M., Bürgler, D. E., Güntherodt, H. J., Suck, J. B. & Audier, M. 1995 The surface structure of icosahedral $Al_{68}Pd_{23}Mn_9$ measured by STM and LEED. *Appl. Phys. A* **61**, 491–501. (doi:10.1007/BF01540250)

47 Pussi, K., Gierer, M. & Diehl, R. D. 2009 The uniaxially aperiodic structure of a thin Cu film on fivefold *i*-Al–Pd–Mn. *J. Phys., Condens. Matter* **21**, 474213. (doi:10.1088/0953-8984/21/47/474213)
48 Krajčí, M. & Hafner, J. 2007 Pseudomorphic quasiperiodic alkali metal monolayers on an i-Al-Pd-Mn surface. *Phys. Rev. B* **75**, 224205. (doi:10.1103/PhysRevB.75.224205)
49 Sharma, H. R. 2009 Structure of the fivefold surface of the Ag-In-Yb icosahedral quasicrystal. *Phys. Rev. B* **80**, 121401(R). (doi:10.1103/PhysRevB.80.121401)
50 Sharma, H. R., Simutis, G., Dhanak, V. R., Nugent, P. J., Cui, C., Shimoda, M., McGrath, R., Tsai, A. P. & Ishii, Y. 2010 Valence band structure of the icosahedral Ag-In-Yb quasicrystal. *Phys. Rev. B* **81**, 104205. (doi:10.1103/PhysRevB.81.104205)
51 McGrath, R., Ledieu, J., Cox, E. J., Haq, S., Diehl, R. D., Jenks, C. J., Fisher, I., Ross, A. R. & Lograsso, T. A. 2002 Quasicrystal surfaces: potential as templates for molecular adsorption. *J. Alloys Compd.* **342**, 432–436. (doi:10.1016/S0925-8388(02)00270-0)
52 Tennant, G. 2001 *Six Sigma: SPC and TQM in manufacturing and services*. Hampshire, UK: Gower.